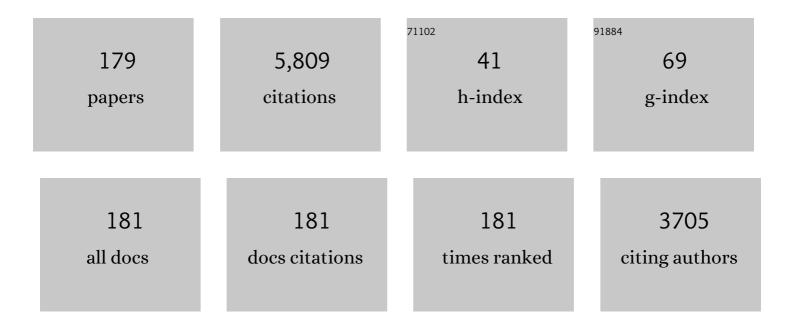
Tokuyuki Teraji

List of Publications by Year in descending order

Source: https://exaly.com/author-pdf/6095245/publications.pdf Version: 2024-02-01



Τοκιινιικι Τερλιι

#	Article	IF	CITATIONS
1	Charge stability of shallow single nitrogen-vacancy centers in lightly boron-doped diamond. Carbon, 2022, 192, 473-481.	10.3	6
2	Loop-gap microwave resonator for millimeter-scale diamond quantum sensor. Materials Today Communications, 2022, , 103488.	1.9	0
3	Effect of surface irregularities on diamond Schottky barrier diode with threading dislocations. Diamond and Related Materials, 2022, 127, 109188.	3.9	4
4	Propagation of dislocations in diamond (111) homoepitaxial layer. Journal of Applied Physics, 2022, 132, .	2.5	5
5	Comprehensive nanoscopic analysis of tungsten carbide/Oxygenated-diamond contacts for Schottky barrier diodes. Applied Surface Science, 2021, 537, 147874.	6.1	2
6	Determining the position of a single spin relative to a metallic nanowire. Journal of Applied Physics, 2021, 129, .	2.5	3
7	Polarization Transfer to External Nuclear Spins Using Ensembles of Nitrogen-Vacancy Centers. Physical Review Applied, 2021, 15, .	3.8	19
8	Long gap spark discharge ignition using a boron-doped diamond electrode. Journal Physics D: Applied Physics, 2021, 54, 405204.	2.8	3
9	Distinguishing dislocation densities in intrinsic layers of pin diamond diodes using two photon-excited photoluminescence imaging. Diamond and Related Materials, 2021, 117, 108463.	3.9	2
10	Boron-Doped Diamond MOSFETs With High Output Current and Extrinsic Transconductance. IEEE Transactions on Electron Devices, 2021, 68, 3963-3967.	3.0	10
11	Equilibrium charge state of NV centers in diamond. Applied Physics Letters, 2021, 119, .	3.3	12
12	Dislocations in chemical vapor deposition diamond layer detected by confocal Raman imaging. Journal of Applied Physics, 2020, 128, .	2.5	17
13	Benchmark for Synthesized Diamond Sensors Based on Isotopically Engineered Nitrogenâ€Vacancy Spin Ensembles for Magnetometry Applications. Advanced Quantum Technologies, 2020, 3, 2000074.	3.9	14
14	Effect of Deep-Defects Excitation on Mechanical Energy Dissipation of Single-Crystal Diamond. Physical Review Letters, 2020, 125, 206802.	7.8	14
15	Spin coherence and depths of single nitrogen-vacancy centers created by ion implantation into diamond via screening masks. Journal of Applied Physics, 2020, 127, 244502.	2.5	4
16	Effect of Annealing Temperature on Performances of Boron-Doped Diamond Metal–Semiconductor Field-Effect Transistors. IEEE Transactions on Electron Devices, 2020, 67, 1680-1685.	3.0	10
17	Comparison of different methods of nitrogen-vacancy layer formation in diamond for wide-field quantum microscopy. Physical Review Materials, 2020, 4, .	2.4	14
18	Ultrapure homoepitaxial diamond films grown by chemical vapor deposition for quantum device application. Semiconductors and Semimetals, 2020, 103, 37-55.	0.7	1

#	Article	IF	CITATIONS
19	dc Magnetometry with Engineered Nitrogen-Vacancy Spin Ensembles in Diamond. Nano Letters, 2019, 19, 6681-6686.	9.1	39
20	High Output Current Boron-Doped Diamond Metal-Semiconductor Field-Effect Transistors. IEEE Electron Device Letters, 2019, 40, 1748-1751.	3.9	17
21	Nonvanishing effect of detuning errors in dynamical-decoupling-based quantum sensing experiments. Physical Review A, 2019, 99, .	2.5	13
22	Apparent delocalization of the current density in metallic wires observed with diamond nitrogen-vacancy magnetometry. Physical Review B, 2019, 99, .	3.2	14
23	Nitrogen-Terminated Diamond Surface for Nanoscale NMR by Shallow Nitrogen-Vacancy Centers. Journal of Physical Chemistry C, 2019, 123, 3594-3604.	3.1	46
24	Detection of Defects in Diamond by Etchâ€Pit Formation. Physica Status Solidi (A) Applications and Materials Science, 2019, 216, 1900247.	1.8	8
25	Triple nitrogen-vacancy centre fabrication by C5N4Hn ion implantation. Nature Communications, 2019, 10, 2664.	12.8	33
26	Microscopic Imaging of the Stress Tensor in Diamond Using in Situ Quantum Sensors. Nano Letters, 2019, 19, 4543-4550.	9.1	51
27	Operations of hydrogenated diamond metal–oxide–semiconductor field-effect transistors after annealing at 500 °C. Journal Physics D: Applied Physics, 2019, 52, 315104.	2.8	13
28	Dislocation analysis of homoepitaxial diamond (001) film by x-ray topography. Japanese Journal of Applied Physics, 2019, 58, 045503.	1.5	12
29	Carbon 1s X-ray photoelectron spectra of realistic samples of hydrogen-terminated and oxygen-terminated CVD diamond (111) and (001). Diamond and Related Materials, 2019, 93, 105-130.	3.9	25
30	Photoelectrical imaging and coherent spin-state readout of single nitrogen-vacancy centers in diamond. Science, 2019, 363, 728-731.	12.6	120
31	One-port SAW resonator on diamond made of isotopically enriched 12C. , 2019, , .		0
32	Ultrahigh Performance Onâ€Chip Single Crystal Diamond NEMS/MEMS with Electrically Tailored Selfâ€Sensing Enhancing Actuation. Advanced Materials Technologies, 2019, 4, 1800325.	5.8	25
33	Spin properties of dense near-surface ensembles of nitrogen-vacancy centers in diamond. Physical Review B, 2018, 97, .	3.2	76
34	High-mobility diamond field effect transistor with a monocrystalline h-BN gate dielectric. APL Materials, 2018, 6, .	5.1	59
35	Precise measurements of diamond lattice constant using Bond method. Japanese Journal of Applied Physics, 2018, 57, 111301.	1.5	21
36	Lattice vibrations of single and multi-layer isotopologic graphene. Carbon, 2018, 140, 449-457.	10.3	4

#	Article	IF	CITATIONS
37	Proximity-Induced Artefacts in Magnetic Imaging with Nitrogen-Vacancy Ensembles in Diamond. Sensors, 2018, 18, 1290.	3.8	18
38	Lithographically engineered shallow nitrogen-vacancy centers in diamond for external nuclear spin sensing. New Journal of Physics, 2018, 20, 083029.	2.9	18
39	Reducing intrinsic energy dissipation in diamond-on-diamond mechanical resonators toward one million quality factor. Physical Review Materials, 2018, 2, .	2.4	17
40	Magnetic noise from ultrathin abrasively deposited materials on diamond. Physical Review Materials, 2018, 2, .	2.4	10
41	Atomic composition of WC/ and Zr/O-terminated diamond Schottky interfaces close to ideality. Applied Surface Science, 2017, 395, 200-207.	6.1	20
42	Displacement current of Au/p-diamond Schottky contacts. Materials Science in Semiconductor Processing, 2017, 70, 207-212.	4.0	1
43	Nitrogen-vacancy centers created by N+ ion implantation through screening SiO2 layers on diamond. Applied Physics Letters, 2017, 110, .	3.3	10
44	Plasma etching phenomena in heavily boron-doped diamond growth. Diamond and Related Materials, 2017, 76, 38-43.	3.9	10
45	Homoepitaxial diamond chemical vapor deposition for ultra-light doping. Materials Science in Semiconductor Processing, 2017, 70, 197-202.	4.0	8
46	Characteristic Luminescence Correlated with Leaky Diamond Schottky Barrier Diodes. Physica Status Solidi (A) Applications and Materials Science, 2017, 214, 1700180.	1.8	11
47	Reducing energy dissipation and surface effect of diamond nanoelectromechanical resonators by annealing in oxygen ambient. Carbon, 2017, 124, 281-287.	10.3	11
48	Protecting a Diamond Quantum Memory by Charge State Control. Nano Letters, 2017, 17, 5931-5937.	9.1	66
49	Charge state stabilization of shallow nitrogen vacancy centers in diamond by oxygen surface modification. Japanese Journal of Applied Physics, 2017, 56, 04CK08.	1.5	46
50	Photoluminescence excitation spectroscopy of SiV ^{â^'} and GeV ^{â^'} color center in diamond. New Journal of Physics, 2017, 19, 063036.	2.9	75
51	Direct determination of the barrier height of Au ohmic-contact on a hydrogen-terminated diamond (001) surface. Diamond and Related Materials, 2017, 73, 182-189.	3.9	14
52	(Invited) Ultrapure Homoepitaxial Diamond Films Grown by Chemical Vapor Deposition. ECS Transactions, 2017, 80, 271-276.	0.5	0
53	Mechanism of reverse current increase of vertical-type diamond Schottky diodes. Journal of Applied Physics, 2017, 122, .	2.5	23
54	Crystalline Diamond Substrates for Power Devices. Journal of the Institute of Electrical Engineers of Japan. 2017, 137, 689-692.	0.0	0

#	Article	IF	CITATIONS
55	Deterministic doping to silicon and diamond materials for quantum processing. , 2016, , .		1
56	Polarization- and frequency-tunable microwave circuit for selective excitation of nitrogen-vacancy spins in diamond. Applied Physics Letters, 2016, 109, .	3.3	23
57	Competition between electric field and magnetic field noise in the decoherence of a single spin in diamond. Physical Review B, 2016, 93, .	3.2	69
58	Reprint of "Imaging of diamond defect sites by electron-beam-induced current― Diamond and Related Materials, 2016, 63, 30-37.	3.9	3
59	Investigation of the silicon vacancy color center for quantum key distribution. Optics Express, 2015, 23, 32961.	3.4	11
60	High-quality and high-purity homoepitaxial diamond (100) film growth under high oxygen concentration condition. Journal of Applied Physics, 2015, 118, .	2.5	47
61	Homoepitaxial diamond film growth: High purity, high crystalline quality, isotopic enrichment, and single color center formation. Physica Status Solidi (A) Applications and Materials Science, 2015, 212, 2365-2384.	1.8	68
62	New application of NV centers in CVD diamonds as a fluorescent nuclear track detector. Physica Status Solidi (A) Applications and Materials Science, 2015, 212, 2641-2644.	1.8	16
63	Direct determination of the barrier height of Ti-based ohmic contact on p-type diamond (001). Diamond and Related Materials, 2015, 60, 117-122.	3.9	26
64	Fluorescence Polarization Switching from a Single Silicon Vacancy Colour Centre in Diamond. Scientific Reports, 2015, 5, 12244.	3.3	13
65	Imaging of diamond defect sites by electron-beam-induced current. Diamond and Related Materials, 2015, 59, 54-61.	3.9	16
66	All-Optical Initialization, Readout, and Coherent Preparation of Single Silicon-Vacancy Spins in Diamond. Physical Review Letters, 2014, 113, 263602.	7.8	216
67	Multiple intrinsically identical single-photon emitters in the solid state. Nature Communications, 2014, 5, 4739.	12.8	232
68	Isotopically varying spectral features of silicon-vacancy in diamond. New Journal of Physics, 2014, 16, 113019.	2.9	85
69	Perfect alignment and preferential orientation of nitrogen-vacancy centers during chemical vapor deposition diamond growth on (111) surfaces. Applied Physics Letters, 2014, 104, .	3.3	134
70	Thermal stabilization and deterioration of the WC/pâ€ŧype diamond (100) Schottkyâ€barrier interface. Physica Status Solidi (A) Applications and Materials Science, 2014, 211, 2363-2366.	1.8	11
71	Isotopic identification of engineered nitrogen-vacancy spin qubits in ultrapure diamond. Physical Review B, 2014, 90, .	3.2	10
72	Diamond Schottky diodes with ideality factors close to 1. Applied Physics Letters, 2014, 105, 133515.	3.3	19

#	Article	IF	CITATIONS
73	Electronic structure of the negatively charged silicon-vacancy center in diamond. Physical Review B, 2014, 89, .	3.2	175
74	Direct observation of the leakage current in epitaxial diamond Schottky barrier devices by conductive-probe atomic force microscopy and Raman imaging. Journal Physics D: Applied Physics, 2014, 47, 355102.	2.8	11
75	lsotopic enrichment of diamond using microwave plasma-assisted chemical vapor deposition with high carbon conversion efficiency. Thin Solid Films, 2014, 557, 231-236.	1.8	6
76	Improved depth resolution of secondary ion mass spectrometry profiles in diamond: A quantitative analysis of the delta-doping. Thin Solid Films, 2014, 557, 222-226.	1.8	21
77	Array of bright silicon-vacancy centers in diamond fabricated by low-energy focused ion beam implantation. Applied Physics Express, 2014, 7, 115201.	2.4	73
78	Indistinguishable Photons from Separated Silicon-Vacancy Centers in Diamond. Physical Review Letters, 2014, 113, 113602.	7.8	333
79	Schottky barrier height and thermal stability of p-diamond (100) Schottky interfaces. Thin Solid Films, 2014, 557, 241-248.	1.8	20
80	Characterization of free-standing single-crystal diamond prepared by hot-filament chemical vapor deposition. Diamond and Related Materials, 2014, 48, 19-23.	3.9	29
81	Model implementation towards the prediction of J(V) characteristics in diamond bipolar device simulations. Diamond and Related Materials, 2014, 43, 34-42.	3.9	26
82	Extending spin coherence times of diamond qubits by high-temperature annealing. Physical Review B, 2013, 88, .	3.2	122
83	Experimental Implementation of Assisted Quantum Adiabatic Passage in a Single Spin. Physical Review Letters, 2013, 110, 240501.	7.8	166
84	Effective Use of Source Gas for Diamond Growth with Isotopic Enrichment. Applied Physics Express, 2013, 6, 055601.	2.4	24
85	Synchronized B and ¹³ C Diamond Delta Structures for an Ultimate In-Depth Chemical Characterization. Applied Physics Express, 2013, 6, 045801.	2.4	17
86	Diamond bipolar device simulation. , 2013, , .		1
87	Strongly coupled diamond spin qubits by molecular nitrogen implantation. Physical Review B, 2013, 88,	3.2	41
88	Chemical Vapor Deposition of ¹² C Isotopically Enriched Polycrystalline Diamond. Japanese Journal of Applied Physics, 2012, 51, 090104.	1.5	13
89	Long coherence time of spin qubits in ¹² C enriched polycrystalline chemical vapor deposition diamond. Applied Physics Letters, 2012, 101, 012405.	3.3	56
90	Local stress distribution of dislocations in homoepitaxial chemical vapor deposite single-crystal diamond. Diamond and Related Materials, 2012, 23, 109-111.	3.9	27

#	Article	IF	CITATIONS
91	Forward tunneling current in {111}-oriented homoepitaxial diamond p–n junction. Diamond and Related Materials, 2012, 21, 33-36.	3.9	3
92	Localized mid-gap-states limited reverse current of diamond Schottky diodes. Journal of Applied Physics, 2012, 111, 104503.	2.5	12
93	High quality pâ€ŧype chemical vapor deposited {111}â€oriented diamonds: Growth and fabrication of related electrical devices. Physica Status Solidi (A) Applications and Materials Science, 2012, 209, 1978-1981.	1.8	6
94	Chemical Vapor Deposition of ¹² C Isotopically Enriched Polycrystalline Diamond. Japanese Journal of Applied Physics, 2012, 51, 090104.	1.5	6
95	Diamonds Utilized in the Development of Single Ion Detector with High Spatial Resolution. Transactions of the Materials Research Society of Japan, 2012, 37, 241-244.	0.2	0
96	Schottky diode architectures on p-type diamond for fast switching, high forward current density and high breakdown field rectifiers. Diamond and Related Materials, 2011, 20, 285-289.	3.9	19
97	Non-destructive detection of killer defects of diamond Schottky barrier diodes. Journal of Applied Physics, 2011, 110, .	2.5	44
98	Hall hole mobility in boron-doped homoepitaxial diamond. Physical Review B, 2010, 81, .	3.2	125
99	Effects of shallow traps on the reverse current of diamond Schottky diode: An electrical transient study. Physica Status Solidi (A) Applications and Materials Science, 2010, 207, 1460-1463.	1.8	2
100	High breakdown voltage Schottky diodes synthesized on pâ€ŧype CVD diamond layer. Physica Status Solidi (A) Applications and Materials Science, 2010, 207, 2088-2092.	1.8	47
101	Extreme dielectric strength in boron doped homoepitaxial diamond. Applied Physics Letters, 2010, 97, .	3.3	160
102	Low-leakage p-type diamond Schottky diodes prepared using vacuum ultraviolet light/ozone treatment. Journal of Applied Physics, 2009, 105, .	2.5	71
103	pâ€ŧype diamond Schottky diodes fabricated by vacuum ultraviolet light/ozone surface oxidation: Comparison with diodes based on wet•hemical oxidation. Physica Status Solidi (A) Applications and Materials Science, 2009, 206, 2082-2085.	1.8	16
104	Highâ€ŧemperature stability of Au/pâ€ŧype diamond Schottky diode. Physica Status Solidi - Rapid Research Letters, 2009, 3, 211-213.	2.4	36
105	P-doped diamond grown on (110)-textured microcrystalline diamond: growth, characterization and devices. Journal of Physics Condensed Matter, 2009, 21, 364204.	1.8	28
106	Electric field breakdown of lateral-type Schottky diodes formed on lightly doped homoepitaxial diamond. Applied Surface Science, 2008, 254, 6273-6276.	6.1	12
107	Deep levels in homoepitaxial boronâ€doped diamond films studied by capacitance and current transient spectroscopies. Physica Status Solidi (A) Applications and Materials Science, 2008, 205, 2179-2183.	1.8	8
108	Ohmic contact for p-type diamond without postannealing. Journal of Applied Physics, 2008, 104, 016104.	2.5	24

#	Article	IF	CITATIONS
109	Characterization of substrate off-angle effects for high-quality homoepitaxial CVD diamond films. Diamond and Related Materials, 2008, 17, 435-439.	3.9	22
110	Characterization of boron doped diamond epilayers grown in a NIRIM type reactor. Diamond and Related Materials, 2008, 17, 1330-1334.	3.9	48
111	Development of Layered Type Single Crystalline Diamond Radiation Detector as an Energy Spectrometer. Journal of Nuclear Science and Technology, 2008, 45, 391-394.	1.3	3
112	Electric Field Breakdown of Lateral Schottky Diodes of Diamond. Japanese Journal of Applied Physics, 2007, 46, L196-L198.	1.5	41
113	Further improvement in high crystalline quality of homoepitaxial CVD diamond. Diamond and Related Materials, 2007, 16, 679-684.	3.9	20
114	Fabrication of diamond p–i–p–i–p structures and their electrical and electroluminescence properties under high electric fields. Diamond and Related Materials, 2007, 16, 112-117.	3.9	7
115	High-performance diamond soft-X-ray detectors with internal amplification function. Diamond and Related Materials, 2007, 16, 1044-1048.	3.9	16
116	Room-temperature growth of single-crystalline TiO2 thin films on nanometer-scaled substrates by dc magnetron sputtering deposition. Journal of Crystal Growth, 2007, 299, 349-357.	1.5	6
117	Effects of vicinal angles from (001) surface on the Boron-doping features of high-quality homoepitaxial diamond films grown by the high-power microwave plasma chemical-vapor-deposition method. Journal of Crystal Growth, 2007, 309, 145-152.	1.5	14
118	Development of a TOF measurement system of charge carrier dynamics in diamond thin films using a UV pulsed laser. Diamond and Related Materials, 2006, 15, 1921-1925.	3.9	8
119	Formation of self-assembled platinum particles on diamond and their embedding in diamond by microwave plasma chemical vapor depositions. Diamond and Related Materials, 2006, 15, 1544-1549.	3.9	9
120	Highly efficient doping of boron into high-quality homoepitaxial diamond films. Diamond and Related Materials, 2006, 15, 602-606.	3.9	68
121	Chemical vapor deposition of homoepitaxial diamond films. Physica Status Solidi (A) Applications and Materials Science, 2006, 203, 3324-3357.	1.8	73
122	Different behaviors of F+ centers due to electron beam irradiations between synthetic sapphire and Be-diffusion-treated natural sapphire. Journal of Crystal Growth, 2006, 292, 546-549.	1.5	2
123	Electrical properties of diamond p–i–p structures at high electric fields. Applied Surface Science, 2005, 244, 310-313.	6.1	8
124	Growth and characterization of P-doped CVD diamond (111) thin films homoepitaxially grown using trimethylphosphine. Applied Surface Science, 2005, 244, 305-309.	6.1	4
125	Improvement in the crystalline quality of homoepitaxial diamond films by oxygen plasma etching of mirror-polished diamond substrates. Journal of Crystal Growth, 2005, 285, 130-136.	1.5	31
126	Impact ionization phenomenon in single-crystalline rutile TiO2. Applied Surface Science, 2005, 244, 394-398.	6.1	2

#	Article	IF	CITATIONS
127	Hillock-Free Homoepitaxial Diamond (100) Films Grown at High Methane Concentrations. Japanese Journal of Applied Physics, 2005, 44, L216-L219.	1.5	23
128	Fabrication of wrinkled carbon nano-films with excellent field emission characteristics. Diamond and Related Materials, 2005, 14, 2074-2077.	3.9	17
129	Development of a charge-carrier drift velocity measurement system in diamonds by using a UV pulse laser. Diamond and Related Materials, 2005, 14, 1992-1994.	3.9	10
130	High-quality homoepitaxial diamond (100) films grown under high-rate growth condition. Diamond and Related Materials, 2005, 14, 1747-1752.	3.9	31
131	High rate growth and electrical/optical properties of high-quality homoepitaxial diamond (100) films. Diamond and Related Materials, 2005, 14, 255-260.	3.9	42
132	High-quality boron-doped homoepitaxial diamond grown by high-power microwave-plasma chemical-vapor deposition. Journal of Applied Physics, 2004, 96, 5906-5908.	2.5	37
133	Response function measurement of layered type CVD single crystal diamond radiation detectors for 14â€,MeV neutrons. Review of Scientific Instruments, 2004, 75, 3581-3584.	1.3	36
134	Homoepitaxial diamond growth by high-power microwave-plasma chemical vapor deposition. Journal of Crystal Growth, 2004, 271, 409-419.	1.5	80
135	Monte Carlo simulations of electron transport properties of diamond in high electric fields using full band structure. Journal of Applied Physics, 2004, 95, 4866-4874.	2.5	40
136	Highly sensitive UV photodetectors fabricated using high-quality single-crystalline CVD diamond films. Diamond and Related Materials, 2004, 13, 858-862.	3.9	71
137	Transport properties of electron-beam and photo excited carriers in high-quality single-crystalline chemical-vapor-deposition diamond films. Journal of Applied Physics, 2004, 96, 7300-7305.	2.5	47
138	Interfacial charge transfer and hole injection in α-NPD organic overlayer–CVD diamond substrate system. Applied Surface Science, 2004, 237, 470-477.	6.1	1
139	Fabrication of nano-sized platinum particles self-assembled on and in CVD diamond films. Applied Surface Science, 2004, 237, 489-494.	6.1	1
140	Interface formation and properties of α-NPD thermally deposited on CVD diamond films. Applied Surface Science, 2003, 216, 106-112.	6.1	4
141	High rate growth and luminescence properties of high-quality homoepitaxial diamond (100) films. Physica Status Solidi A, 2003, 198, 395-406.	1.7	43
142	Hydrogen-related structural changes on CVD diamond (1 0 0) surfaces by ultra-high-vacuum annealing. Applied Surface Science, 2003, 216, 59-64.	6.1	3
143	Field-induced effects of implanted Ga on high electric field diamond devices fabricated by focused ion beam. Applied Surface Science, 2003, 216, 65-71.	6.1	10
144	Electron emissions from CVD diamond surfaces. Diamond and Related Materials, 2003, 12, 434-441.	3.9	20

9

#	Article	IF	CITATIONS
145	Characterization of phosphorus doped CVD diamond films by cathodoluminescence spectroscopy and topography. Diamond and Related Materials, 2003, 12, 20-25.	3.9	17
146	Ohmic Contact Formation for N-Type Diamond by Selective Doping. Japanese Journal of Applied Physics, 2003, 42, L882-L884.	1.5	37
147	Charge transfer between thermally deposited α-naphthyl-phenyl-diamine and chemical-vapor-deposited homoepitaxial diamond films. Applied Physics Letters, 2003, 83, 4776-4778.	3.3	1
148	Characterization of α-NPD Thermally Deposited on Hydrogen-Terminated Single-Crystal Chemical-Vapor-Deposited Diamond Films. Japanese Journal of Applied Physics, 2003, 42, 5233-5238.	1.5	4
149	Characterization of Organic Material .ALPHANaphthyl Phenyl Diamine Deposited on Chemical Vapor Deposition Diamond Films. Shinku/Journal of the Vacuum Society of Japan, 2003, 46, 229-232.	0.2	Ο
150	Transport Properties of Photo-Excited Carriers in Chemical-Vapor-Deposited Singlecrystalline Diamond using a Short Pulse UV Laser. Shinku/Journal of the Vacuum Society of Japan, 2003, 46, 222-224.	0.2	0
151	Field-induced Effects of Residual Gallium Atoms on High-electric-field Diamond Device Structures Fabricated by Focused Ion Beam. Shinku/Journal of the Vacuum Society of Japan, 2003, 46, 225-228.	0.2	Ο
152	The Effect of Defects Created near Diamond Film Surface on Cathodoluminescence Intensity. Shinku/Journal of the Vacuum Society of Japan, 2003, 46, 466-468.	0.2	0
153	Low-Temperature Morphology Changes of Platinum Thin Films Deposited on Chemical-Vapor-Deposited Diamond Surfaces. Shinku/Journal of the Vacuum Society of Japan, 2003, 46, 703-707.	0.2	0
154	Appearance of n-Type Semiconducting Properties of cBN Single Crystals Grown at High Pressure. Japanese Journal of Applied Physics, 2002, 41, L109-L111.	1.5	74
155	Growth of high-quality homoepitaxial CVD diamond films at high growth rate. Journal of Crystal Growth, 2002, 235, 287-292.	1.5	61
156	Lattice location of phosphorus in n-type homoepitaxial diamond films grown by chemical-vapor deposition. Applied Physics Letters, 2001, 79, 3068-3070.	3.3	42
157	Low temperature excitation spectrum of phosphorus in diamond. Diamond and Related Materials, 2001, 10, 444-448.	3.9	37
158	Phonon-assisted electronic transitions in phosphorus-doped n-type chemical vapor deposition diamond films. Diamond and Related Materials, 2001, 10, 439-443.	3.9	27
159	Effect of Magnetic Field on Phosphorus Centre in Diamond. Physica Status Solidi A, 2001, 186, 291-295.	1.7	6
160	Impact Excitation of Carriers in Diamond under Extremely High Electric Fields. Japanese Journal of Applied Physics, 2001, 40, L715-L717.	1.5	24
161	Boron-Doped Diamond Film Homoepitaxially Grown on High-Quality Chemical-Vapor-Deposited Diamond (100). Japanese Journal of Applied Physics, 2001, 40, 4145-4148.	1.5	14
162	The Electronic Structure of Phosphorus in n-Type CVD Diamond Films: Revised. Physica Status Solidi A, 2000, 181, 11-16.	1.7	12

#	Article	lF	CITATIONS
163	Ohmic Contacts for Phosphorus-Doped n-Type Diamond. Physica Status Solidi A, 2000, 181, 129-139.	1.7	15
164	Electronic transitions of electrons bound to phosphorus donors in diamond. Solid State Communications, 2000, 113, 577-580.	1.9	75
165	Phosphorus-doped chemical vapor deposition of diamond. Diamond and Related Materials, 2000, 9, 935-940.	3.9	193
166	Ga Ohmic contact for n-type diamond by ion implantation. Applied Physics Letters, 2000, 76, 1303-1305.	3.3	16
167	Electronic states of phosphorus in diamond. Diamond and Related Materials, 2000, 9, 948-951.	3.9	66
168	Temperature dependent spectroscopic study of the electronic structure of phosphorus in n-type CVD diamond films. Diamond and Related Materials, 2000, 9, 952-955.	3.9	18
169	Electrical Contacts for n-Type Diamond. Japanese Journal of Applied Physics, 1999, 38, L1096-L1098.	1.5	23
170	Low-temperature spectroscopic study ofn-type diamond. Physical Review B, 1999, 59, 14852-14855.	3.2	69
171	Electronic States of Boron and Phosphorus in Diamond. Physica Status Solidi A, 1999, 174, 39-51.	1.7	74
172	Photocurrent and optical absorption spectroscopic study of n-type phosphorus-doped CVD diamond. Diamond and Related Materials, 1999, 8, 882-885.	3.9	11
173	Ideal Ohmic contact to n-type 6H-SiC by reduction of Schottky barrier height. Applied Physics Letters, 1997, 71, 689-691.	3.3	44
174	Pinning-controlled ohmic contacts: application to SiC(0001). Applied Surface Science, 1996, 107, 218-221.	6.1	11
175	Reply to â€~â€~Comment on â€~A theory on the xâ€ray sensitivity of a silicon surfaceâ€barrier detector including thermal chargeâ€diffusion effect' '' [J. Appl. Phys. 72, 3363 (1992)]. Journal of Applied Physics, 1 1463-1464.	a .9 23 , 74,	0
176	A theory on the xâ€ray sensitivity of a silicon surfaceâ€barrier detector including a thermal chargeâ€diffusion effect. Journal of Applied Physics, 1992, 72, 3363-3373.	2.5	15
177	Evidence against existing x-ray-energy response theories for silicon-surface-barrier semiconductor detectors. Physical Review A, 1992, 46, R3024-R3027.	2.5	54
178	Near-Surface Defects in Boron-Doped Diamond Schottky Diodes Studied From Capacitance Transients. Applied Physics Express, 0, 1, 035003.	2.4	12
179	Creation of multiple NV centers by phthalocyanine ion implantation. Applied Physics Express, 0, , .	2.4	0